A fluorescent turn-on probe for Hg^{2+} with a high contrast designed by manipulating functional groups tethered to naphthalimide

Yuka Shinohara, Koji Tsukamoto*, Hatsuo Maeda

School of Pharmacy, Hyogo University of Health Sciences, 1-3-6 Minatojima, Chuo-ku, Kobe, 650-8530, Japan

ABSTRACT

Based on the concept provided by our previous work on a fluorescent Cd^{2+} probe, a fluorescent turn-on Hg^{2+} probe with a high contrast was designed through manipulating functional groups tethered to naphthalimide. With carbamoylmethylamino and bis[2-(ethylthio)ethyl]amino groups as tethering functionalities, **1** worked as a useful fluorescent probe in a high selective and sensitive manner over the pH range between 6 and 8 with a detection limit at 2.8 nM (estimated at a pH of 7.2). Comparison of the probe performance of **1** with that of **2** merely with bis[2-(ethylthio)ethyl]amino group suggested that both of the tethering groups exhibited their abilities to chelate with Hg^{2+}, and yet the carbamoylmethylamino group also functioned as a fluorescent off-on switch through a photoinduced electron transfer mechanism. Thus, **1** found a practical utility as an Hg^{2+} probe in analysis of river as well as tap samples without any tedious pretreatments.

1. Introduction

In spite of the fact that mercury (Hg) is well recognized as a highly toxic heavy metal, bringing about damage to some organelles in many organs [1–3] by inducing negative effects such as disturbance in cellular functions and reactive oxygen species (ROS) production [4,5], the heavy metal has been discharged by industrial and agricultural activities [3,6]. Hence, its management has been drawing a great attention all over the world, and severely regulated through the Minamata Convention [6]. In addition, a mechanism for the negative effects of Hg on the health of human and other organisms is not fully understood. These contexts have prompted to develop fluorescent probes as a facile, sensitive, and selective detection technique for monitoring in vivo and environmental Hg^{2+} [3,7].

From the standing point of a fluorescence mechanism, fluorescent probes with changes of their fluorescence intensities are categorized into two groups: a "turn-on" or "turn-off" type of probes. The former provides fluorescent responses only after reaction with a target substance, while the latter emits fluorescence as a background response, which is quenched in a manner dependent on concentration of an analyte. As for a "turn-on" probe with its essentially low background signal, the following featuring points are envisioned: a target analyte in a minute amount would be imaged even in biological samples; a use of several probes chosen wisely would allow simultaneous analysis of their target molecules [3,7]. Moreover, it is likely that fluorometry with a

"turn-off" probe suffers from false positives [3], and hence the former would be preferred to the latter as a tool for sensitive and selective analysis. Although a large number of fluorescent probes for Hg^{2+} have been developed so far [3,7–32], some of them are "turn-off" probes accompanied by their mechanism-based problems, and the others often have a drawback that fluorescent background signals are relatively high, namely, insufficiently quenched in the absence of Hg^{2+}, even though a "turn-on" fluorescent mechanism is invoked. Thus, it is still a challenge to establish a concept allowing versatile molecular design of fluorescent "turn-on" probes for Hg^{2+} with a background signal quenched as effectively as possible.

With this view in hand, we paid our attention to previously reported Cd^{2+} probe **3** (Fig. 1) with carbamoylmethylamino groups tethered to naphthalimide, to design a fluorescent Hg^{2+} probe. The pendant groups in **3** function not only as Cd^{2+} chelators but also as fluorescent off-on switches [33]. Since protonation of the amino groups in the pendant groups is suppressed due to an electron-withdrawing property of the adjacent carbamoyl groups, photoinduced electron transfer (PET) from the amino groups onto the naphthalimide moiety occurs even under neutral conditions, leading into sufficiently quenching the fluorescence emission from the naphthalimide as its background responses. In contrast, the observed PET quenching is canceled in the presence of Cd^{2+} through the chelation of the amino groups as well as the carbamoyl groups to the metal ion, allowing **3** to exhibit the fluorescence signal from the naphthalimide. The observed performance of **3** as a Cd^{2+}
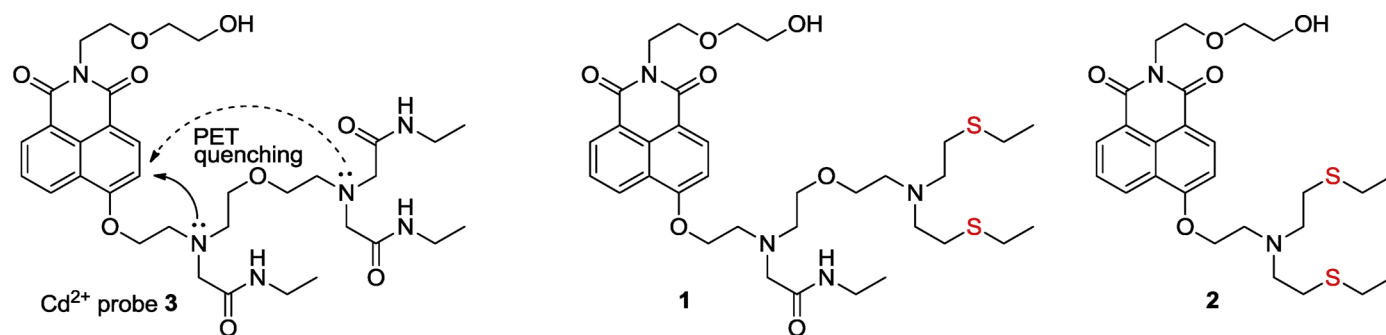
---

* Corresponding author.
  E-mail address: kotukamoto@huhs.ac.jp (K. Tsukamoto).

Fig. 1. Compound **1** designed as an Hg^{2+} probe through the concept brought by the "turn-on" mechanism of previously reported **3** as a Cd^{2+} probe, and **2** that was useful to shed light on the important role of the carbamoylmethylamino group on **1**.

probe has provided the concept that a fluorescent turn-on Hg^{2+} probe in a high-contrast manner would be designed through manipulating functional groups tethered to naphthalimide. Herein, we designed **1** by changing the two terminal carbamoylmethyl groups of **3** into two 2-(ethylthio)ethyl groups as selective chelators toward Hg^{2+} (Fig. 1), and demonstrated its performance and practical utility as a fluorescent "turn-on" probe for Hg^{2+} with high sensitivity and selectivity, quite low background signal, and large increasing on its fluorescent signal. We shed light on a role of the carbamoylmethylamino group in **1** by comparison in probe performance between **1** and **2** lacking the carbamoylmethylamino group as a tethering group to naphthalimide (Fig. 1).

2. Experimental section

2.1. Synthesis

2.1.1. General

IR absorption spectra were measured with a JASCO FT/IR-4100 spectrometer using KBr powder, and only noteworthy absorptions are depicted in the lists of the physical data for each compound. ^{1}H and ^{13}C NMR spectra were measured with a Bruker AVANCE III HD NMR spectrometer (600 MHz and 151 MHz, respectively). Chemical shifts of ^{1}H and ^{13}C NMR are expressed as ppm downfield from tetramethylsilane used as an internal standard ($\delta = 0$ ppm). High resolution mass spectra were measured on a Bruker micrOTOF-Q mass spectrometer by an electrospray ionization time-of-flight (ESI-TOF) method. Column chromatography was carried out by using silica gel 60 (spherical, Kanto Chemical Co., Japan). Compounds **4** and **5** (Scheme 1) were prepared as previously reported [33]. Reactions were performed under an atmosphere of Ar, unless otherwise noted.

2.1.2. Synthesis of 1

To a solution of **4** (1.54 g, 2.90 mmol) in acetonitrile (65 mL), *N*-ethyl-2-bromoacetamide (813 mg, 4.90 mmol) and potassium carbonate (677 mg, 4.90 mmol) were added at room temperature, and stirred under reflux for 4.5 h. The mixture was cooled to room temperature, filtered, and evaporated. The residue was purified by column chromatography on silica gel with CHCl$_3$/methanol/28% aqueous NH$_3$ solution (400:20:1) to afford crude yellow oil (1.74 g). The crude oil (100 mg) was dissolved in trifluoroacetic acid (1.0 mL) at 0 °C, and stirred in the

air at room temperature for 1 h. The resulting mixture was basified with 2 M aqueous NaOH solution and extracted with CHCl$_3$ three times. The combined organic layers were dried over Na$_2$SO$_4$, and evaporated to dryness. The residue was dissolved in acetonitrile (3 mL), and a solution of (2-bromoethylsulfanyl)ethane (85 mg, 0.50 mmol) in acetonitrile (1 mL) and potassium carbonate (70 mg, 0.51 mmol) were added to the solution with stirring. The mixture was stirred under reflux for 3 h, then cooled to room temperature, filtered, and evaporated. The residue was purified by column chromatography on silica gel with CHCl$_3$/methanol/28% aqueous NH$_3$ solution (400:10:1) to give the desired product including a few impurities. The product was subjected to additional silica gel chromatography with CHCl$_3$/methanol/28% aqueous NH$_3$ solution (400:10:1) to afford pure **1** (28 mg, 24% for three steps) as pale yellow oil.

^{1}H NMR (600 MHz, CDCl$_3$): $\delta = 8.63$ (dd, $J = 7.3, 1.2$ Hz, 1 H), 8.56 (d, $J = 8.3$ Hz, 1 H), 8.55 (dd, $J = 8.3, 1.2$ Hz, 1 H), 7.74 (dd, $J = 8.3, 7.3$ Hz, 1 H), 7.53 (t, $J = 6.0$ Hz, 1 H), 7.04 (d, $J = 8.3$ Hz, 1 H), 4.44 (t, $J = 5.7$ Hz, 2 H), 4.34 (t, $J = 5.2$ Hz, 2 H), 3.86 (t, $J = 5.7$ Hz, 2 H), 3.72–3.65 (m, 4 H), 3.58 (t, $J = 5.1$ Hz, 2 H), 3.53 (t, $J = 6.1$ Hz, 2 H), 3.38 (s, 2 H), 3.26 (t, $J = 5.2$ Hz, 2 H), 3.16 (qd, $J = 7.3, 6.0$ Hz, 2 H), 2.92 (t, $J = 5.1$ Hz, 2 H), 2.75–2.72 (m, 4 H), 2.70 (t, $J = 6.1$ Hz, 2 H), 2.60–2.57 (m, 4 H), 2.53 (q, $J = 7.4$ Hz, 4 H), 1.25 (t, $J = 7.4$ Hz, 6 H), 0.94 ppm (t, $J = 7.3$ Hz, 3 H);

^{13}C NMR (151 MHz, CDCl$_3$): $\delta = 171.04, 164.76, 164.17, 159.89, 133.65, 131.94, 129.55, 128.57, 126.21, 123.47, 122.41, 115.25, 106.00, 72.25, 70.06, 69.16, 68.55, 67.29, 61.88, 59.67, 55.82, 54.79$ (2C), $54.73, 53.64, 39.42, 33.82, 29.54$ (2C), 26.32 (2C), 14.93 (2C), 14.89 ppm;

IR (KBr): $\tilde{\nu} = 3330$ (broad), 2960, 2926, 2871, 1695, 1656, 1593, 1581 cm^{-1};

HRMS m/z ([M + H]$^+$): Calcd for 693.3350; Found 693.3350, ([M + Na]$^+$): Calcd for 715.3170; Found 715.3170.

2.1.3. Synthesis of 2

To a solution of **5** (200 mg, 0.490 mmol) in DMSO (2.5 mL), sodium azide (48 mg, 0.74 mmol) was added and stirred at 60 °C for 4 h. After cooling to room temperature, water (approximately 10 mL) was added, and then the precipitate was collected by filtration, washed with water three times, and dried in vacuo to afford a crude yellow powder (168 mg). Next, hydrogenation of the obtained crude (168 mg)
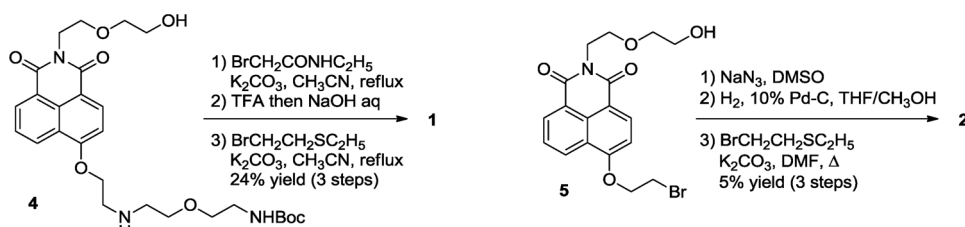
Scheme 1. Synthetic routes for **1** and **2**.

dissolved in THF/methanol (1:2, 6 mL) was carried out over 10% Pd-C (68 mg) under a medium pressure condition of hydrogen (0.4 MPa) for 2 h. After removal of Pd-C by filtration, the filtrate was evaporated to give the crude amine as a yellow foam solid (88 mg). To a solution of the crude (88 mg) in DMF (0.6 mL), a solution of (2-bromoethylsulfanyl)ethane (86 mg, 0.51 mmol) in DMF (0.6 mL) and potassium carbonate (71 mg, 0.51 mmol) were added at room temperature, and stirred at 60 °C overnight. After cooling to room temperature, the resulting mixture was quenched with water, and extracted with $CHCl_3$ three times. The combined organic layers were dried over Na_2SO_4, filtered, and evaporated to dryness. The residue was purified by column chromatography on silica gel with $CHCl_3$/methanol (40:1) to give the desired product, including impurities. Further purification with column chromatography on silica gel with $CHCl_3$/acetone (5:1) was carried out to afford pure **2** as yellow oil (13 mg, 5.1% for three steps).

^{1}H NMR (600 MHz, $CDCl_3$): δ = 8.62 (dd, J = 7.3, 1.1 Hz, 1 H), 8.57 (dd, J = 8.3, 1.1 Hz, 1 H), 8.56 (d, J = 8.3 Hz, 1 H), 7.71 (dd, J = 8.3, 7.3 Hz, 1 H), 7.06 (d, J = 8.3 Hz, 1 H), 4.44 (t, J = 5.7 Hz, 2 H), 4.36 (t, J = 5.7 Hz, 2 H), 3.86 (t, J = 5.7 Hz, 2 H), 3.72–3.65 (m, 4 H), 3.16 (t, J = 5.7 Hz, 2 H), 2.92–2.89 (m, 4 H), 2.71–2.68 (m, 4 H), 2.57 (q, J = 7.4 Hz, 4 H), 1.25 ppm (t, J = 7.4 Hz, 6 H);

^{13}C NMR (151 MHz, $CDCl_3$): δ = 164.88, 164.27, 160.18, 133.76, 131.86, 129.55, 128.96, 126.02, 123.54, 122.27, 114.95, 106.04, 72.23, 68.57, 68.03, 61.89, 55.00 (2C), 52.78, 39.39, 29.85 (2C), 26.38 (2C), 14.92 (2C) ppm;

IR (KBr): $\tilde{\nu}$ = 3480 (broad), 2959, 2925, 2869, 1695, 1656, 1593, 1581 cm^{-1};

HRMS m/z ([M + H]$^+$): Calcd for 521.2138; Found 521.2139, ([M + Na]$^+$): Calcd for 543.1958; Found 543.1961.

2.2. Spectroscopic analysis

2.2.1. General

All reagents and solvents in spectroscopic analysis were of the highest quality purchased from Nacalai Tesque (Japan), Sigma-Aldrich Co. (USA), and Wako Pure Chemical Industries (Japan), and used without purification. As metal reagents, $HgCl_2$, $CrCl_3 \cdot 6H_2O$, $MnCl_2 \cdot 4H_2O$, $FeCl_3 \cdot 6H_2O$, $CoCl_2 \cdot 6H_2O$, $NiCl_2 \cdot 6H_2O$, $CuCl_2 \cdot 2H_2O$, Zn $(NO_3)_2 \cdot 6H_2O$, $Pb(NO_3)_2$, $AgNO_3$, $CdCl_2 \cdot 2.5H_2O$, $MgCl_2 \cdot 6H_2O$, $CaCl_2 \cdot 2H_2O$, $NaNO_3$, and KNO_3 were used, unless otherwise noted. Water was purified using a Millipore Milli-Q Advantage A10 system coupled with a Millipore Elix Essential 5 UV water purification system (Merck Millipore, USA). As a pH 7.2 buffer, 50 mM phosphate buffer was used. UV/Vis absorption spectra were measured on a Shimadzu UV-2550 UV–vis Spectrophotometer (Shimadzu Corporation, Japan). All fluorescence spectra were recorded on a JASCO FP-750 spectrofluorometer equipped with an ETC-272 Peltier thermostatted cell holder (JASCO Corporation, Japan). Both the slit widths for excitation and emission monochrometers were 5 nm. Each of spectral data was obtained with individual three trials, unless otherwise noted.

2.2.2. Fluorometric analysis

Stock solutions of compounds **1** and **2** in DMSO, and metal ions (Hg^{2+}, Cr^{3+}, Mn^{2+}, Fe^{3+}, Co^{2+}, Ni^{2+}, Cu^{2+}, Zn^{2+}, Pb^{2+}, Ag^+, and Cd^{2+}) in water were prepared at a concentration of 5 mM. Stock solutions of the other metal ions (Mg^{2+}, Ca^{2+}, Na^+, and K^+) in water were prepared at a concentration of 50 mM. Fluorometric samples were provided by diluting the stock solution(s) with a buffer solution in a $1 \times 1 \times 4.5$ cm quartz cell. Thus the obtained solution of each compound in the absence or presence of the metal ions was subjected to fluorometric analysis with stirring at 25 °C. It should be mentioned here that the fluorescent performances of **1** and **2** were not affected at all in aqueous media containing DMSO with less than 10% (Fig. S1).

2.2.3. Measurement of fluorescence quantum yields

Fluorescence quantum yields were calculated using the following

equation according to a relative method with reference to the quantum yield of quinine bisulfate in 0.5 M H_2SO_4 aqueous solution (ϕ_r = 0.546) [34].

$$\phi_s = \phi_r \frac{A_r D_s n_s^2}{A_s D_r n_r^2}$$

where s denotes the sample, r denotes the reference, ϕ is the quantum yield, A is the absorbance at the excitation wavelength of the sample, D is the area under the fluorescence emission spectrum, and n is the refractive index. Absorption spectra were measured with 5 μM solution of a fluorescent sample in pH 7.2 phosphate buffer, and fluorescence spectra were measured with 5 μM solution of the sample excited at the wavelength of its maximum absorbance in pH 7.2 phosphate buffer. Absorption and fluorescence spectra of quinine bisulfate solution were also measured at a concentration of 5 μM. The excitation wavelength in the fluorescence measurement of quinine bisulfate was the same to that of the fluorescent sample.

2.2.4. Dependency on pH

The experiments at various pH values were carried out in the following solutions: 50 mM citric acid–sodium citrate buffer (pH 3.0), 50 mM AcOH–AcONa buffer (pH 4.0, 5.0), 50 mM phosphate buffer (pH 6.0–8.0), and 50 mM $NaHCO_3$–Na_2CO_3 buffer (pH 9.2, 10.0). All samples were prepared by adding the stock solution of **1** in DMSO into buffer, and hence fluorescent measurements were carried out in aqueous media containing 0.1% (v/v) DMSO.

2.2.5. Practical analysis of water samples

River water was collected at a point (lat. 34°43′24.0″ N and long. 135°16′35.2″ E) of Tenjo River, Kobe, Japan. As tentatively practical samples, the mixed solutions of pH 7.2 phosphate buffer (50 mM) and tap or river water (1:1, v/v) were spiked with Hg^{2+} at various concentrations between 0.05–2 μM. A calibration curve for Hg^{2+} was obtained by the fluorometry with four standard solutions of **1** (5 μM) containing Hg^{2+} at different concentrations (0.05, 0.25, 0.5, 1 μM) in mixtures of pH 7.2 phosphate buffer (50 mM) and water (1:1, v/v). All samples were prepared by adding the stock solution of **1** in DMSO into buffer, and hence fluorescent measurements were carried out in aqueous media containing 0.1% (v/v) DMSO.

3. Results and discussion

3.1. Probe performance of **1** and **2**

Compounds **1** and **2** were synthesized as depicted in Scheme 1, and subjected to absorption spectroscopy (Fig. S2). The spectra of **1** and **2** in pH 7.2 phosphate buffer were essentially the same: they exhibited the maximum absorption wavelengths (λ_{max}) at 375 nm, and addition of Hg^{2+} to their solutions gave minute shifts of the maximum absorption wavelengths of **1** and **2** to 370 nm and 372 nm, respectively. Fig. 2 shows their fluorometry in the absence and presence of Hg^{2+} in pH 7.2 phosphate buffer. As expected, fluorescence of the naphthalimide group in **1** was efficiently quenched (ϕ = 0.004), and addition of 1 equiv of Hg^{2+} into its solution recovered fluorescence emission (ϕ = 0.81). The increasing ratio of its fluorescence quantum yield with or without Hg^{2+} was approximately 200 times, demonstrating that **1** worked as an Hg^{2+} probe in a high-contrast manner. On the other hand, fluorescence of the fluorophore in **2** was not completely quenched (ϕ = 0.085), though its fluorescence emission was recovered by addition of 1 equiv of Hg^{2+} (ϕ = 0.42). The comparison in probe performance between **1** and **2** was informative to evaluate the functions of the tethering groups on naphthalimide, demonstrating that (1) the carbamoylmethylamino group in **1** is essential to quenching fluorescence of naphthalimide at an almost baseline level, (2) coordination of the carbamoylmethylamino group in **1** to Hg^{2+} cancels the PET quenching by its N atom, (3) the bis
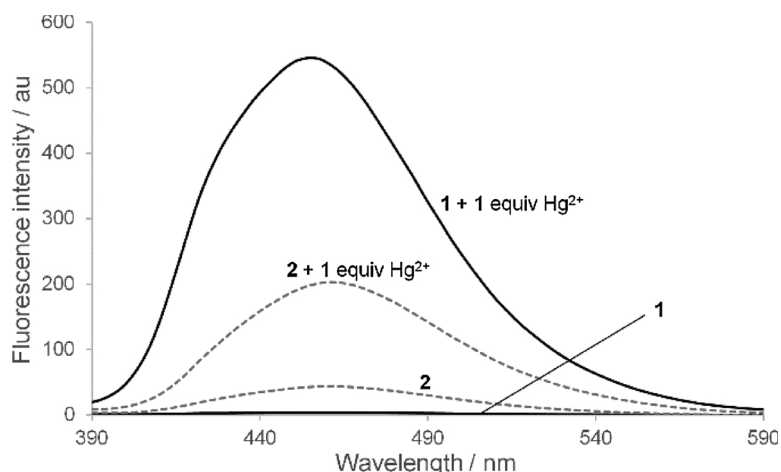
Fig. 2. Fluorescence spectral changes of **1** and **2** (5 μM) upon addition of Hg^{2+} (1 equiv). The data were collected in pH 7.2 phosphate buffer containing 0.1% (v/v) DMSO at λ_{ex} = 370 nm.

[2-(ethylthio)ethyl]amino group itself exerts an Hg^{2+}-binding ability in both of **1** and **2**, and (4) the bis[2-(ethylthio)ethyl]amino group does not quench the fluorescence emission from naphthalimide as much as the carbamoylmethylamino group combined with the bis[2-(ethylthio)ethyl]amino group under the conditions. Therefore, manipulation of functional groups tethered to naphthalimide led to a successful design of **1** as a fluorescent turn-on probe for Hg^{2+}.

The influence of pH on the fluorescent properties of **1** and **2** was investigated as well (Fig. 3). The fluorescence of **1** was almost completely quenched at pH higher than 6, while **2** just underwent weaker quenching than **1** even at a high pH region. This result indicates that the electron-withdrawing effect of the carbamoylmethyl group in **1** suppressed protonation of the adjacent amino group over these pH range, leading to the effective PET quenching [33]. As the pH value of the media was lower than 6, the fluorescence intensities of **1** and **2** became larger. This phenomenon was attributed to the cessation of the PET quenching by protonation of the amino groups [33]. However, the quenching in **1** and **2** was not totally canceled under acidic conditions, which could be ascribed to a heavy atom effect of intramolecular sulfur atoms in ethylthio groups [35]. This explanation is supported by the previously reported data obtained on **6** (Fig. 4), which is a lack of the ethylthio groups in **2**: the fluorescent intensity of **6** was much stronger than that of **2** over a pH range lower than 9 (the fluorescence quantum yield of **6** was 0.54 at pH 7.2) [33].

As for fluorescent intensity in the presence of Hg^{2+}, an interesting
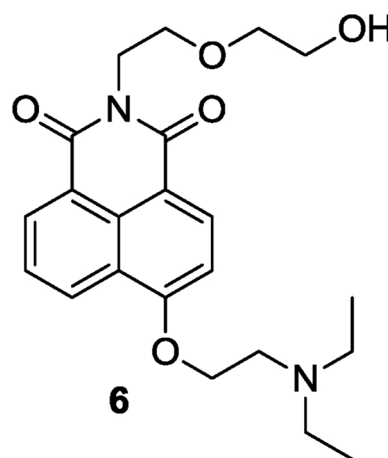

Fig. 4. Compound **6** informative for evaluating the function of the ethylthio groups in **2**.

pH-dependency was observed. Over the pH range between 3 and 8, Hg^{2+} turned on the fluorescence switch of **1** and **2**, bringing out almost full fluorescent responses from the probes. At pH higher than 9, the fluorescent responses of **1** and **2** toward Hg^{2+} were lower than those obtained under the neutral conditions. This is probably because HgO

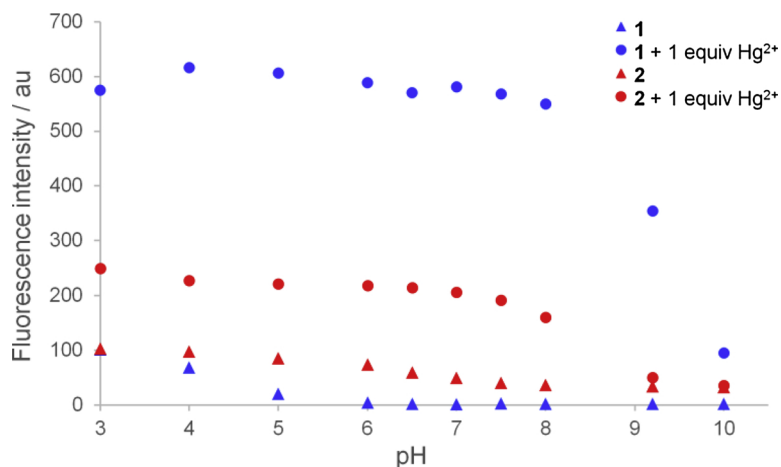**Fig. 3.** Dependency of the fluorescence intensities of **1** and **2** (5 μM) on pH in the absence or presence of 1 equiv of Hg^{2+}. The data were collected at λ_{ex} = 370 nm and λ_{em} = 455 nm.

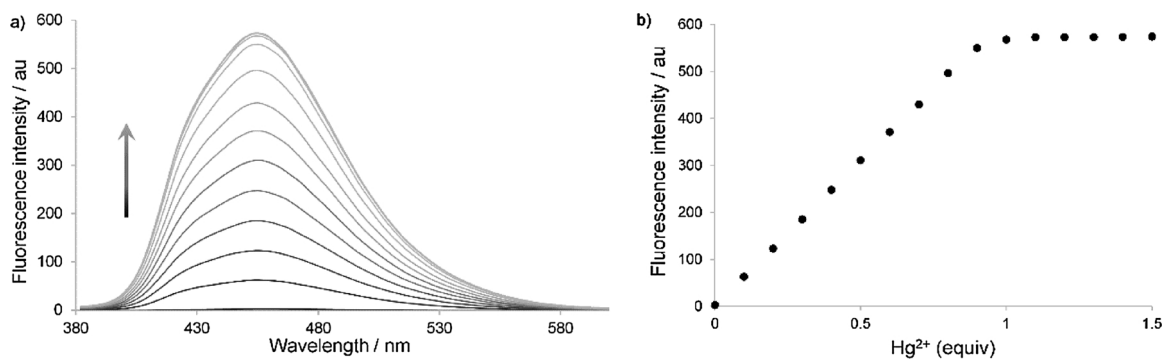**Fig. 5.** (a) Gradual change in the fluorescence spectrum of **1** (5 μM) by the continuous addition of Hg^{2+} up to 1.5 equiv (7.5 μM). (b) A plot of the fluorescence intensities at λ_{em} = 455 nm obtained from the reaction of **1** (5 μM) with Hg^{2+} as a function of the amount of Hg^{2+}. The data were collected in pH 7.2 phosphate buffer containing 0.1% (v/v) DMSO at λ_{ex} = 370 nm.

was formed by a reaction of Hg^{2+} with OH^- in a basic aqueous solution [36], leading to decrease in the concentration of Hg^{2+}. Hence, it was demonstrated that **1** worked well as a fluorescent turn-on probe for Hg^{2+} over the pH range between 6 and 8.

3.2. Fluorometric titration and stoichiometry in the reaction of 1 with Hg^{2+}

Since **1** displayed its sensing ability as an Hg^{2+} probe, we investigated the fluorescent property of **1** in more detail. At first, a titration experiment of **1** with Hg^{2+} was carried out by fluorometry (Fig. 5). Upon addition of Hg^{2+} over the concentration range between 0.1 and 1 equiv, the fluorescent signal of **1** increased with a linear relationship, and reached a plateau at 1 equiv of Hg^{2+}. Furthermore, a Job's plot of an increase in the fluorescence intensity by the reaction of **1** with Hg^{2+} showed a maximum at a mole fraction {[**1**]/([**1**] + [Hg^{2+}])} of 0.5 (Fig. 6). These results clarified formation of the 1:1 complex of **1** with Hg^{2+}, which was also indicated by ^1H NMR spectral analysis. In a titration of **1** (2 mM) with Hg^{2+} in the mixed solvent of D_2O and DMSO-d_6 (1:1, v/v) monitored by ^1H NMR spectroscopy, addition of Hg^{2+} up to 1 equiv induced the spectral change for **1**, and the addition beyond 1 equiv of Hg^{2+} showed no further change in the spectra of **1** (Fig. S3). Formation of the 1:1 complex (**1**-Hg^{2+}) was confirmed by ESI-TOF mass spectrometry as well. When a solution of **1** and 1 equiv of $Hg(OAc)_2$ in aqueous acetonitrile was subjected to the mass spectrometry, a series of the isotopic peaks of complex **1**-Hg^{2+} was observed side by side with 0.5 mass unit intervals, indicating that the observed species was a divalent ion, and the major peak at *m/z* 447.1487 was assigned to $[M + {}^{202}Hg]^{2+}$ (Fig. S4).

3.3. Detection limit

The detection limit of Hg^{2+} by the fluorometric method with **1** in pH 7.2 phosphate buffer was estimated to be 2.8 nM from $3\sigma/S$, where σ was the standard deviation of the fluorescence intensity on ten blank measurements (Table S1), and S is the slope in a plot of the fluorometric titration of **1** with Hg^{2+} (Fig. S5). The value is lower than the detection limits reported so far on a number of the fluorescent Hg^{2+} probes (Table S2), and this observation would allow **1** to work for sensitive detection of Hg^{2+}.

3.4. Metal-ion selectivity

The effects by various metal ions (5 μM Cr^{3+}, Mn^{2+}, Fe^{3+}, Co^{2+}, Ni^{2+}, Cu^{2+}, Zn^{2+}, Pb^{2+}, Ag^+ and Cd^{2+}, 0.1 mM Mg^{2+}, Ca^{2+}, Na^+ and K^+) in pH 7.2 phosphate buffer were investigated (Fig. 7). The examined metal ions, except for Ag^+, did not prevent **1** from showing response toward Hg^{2+} at essentially the same levels to those just in the presence of Hg^{2+}. Addition of 5 μM Ag^+ caused a slight decrease in the fluorescent enhancement of **1** toward 5 μM Hg^{2+}. However, the fluorescent response of **1** toward Hg^{2+} was sufficiently retained to detect Hg^{2+} even in the presence of Ag^+. Therefore, **1** functions as a fluorescent probe for highly selective detection of Hg^{2+}.

3.5. Practical analysis for Hg^{2+} using probe 1 in water samples

It was examined whether **1** could find a practical utility as a fluorescent turn-on probe for analysis of Hg^{2+} in real samples or not.

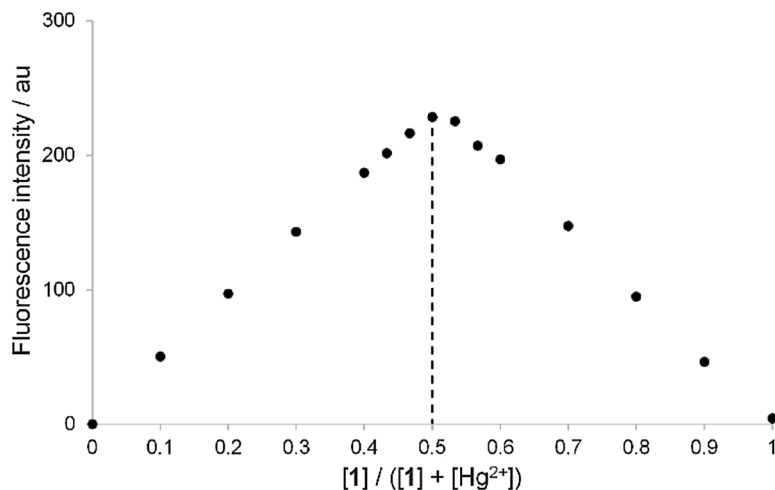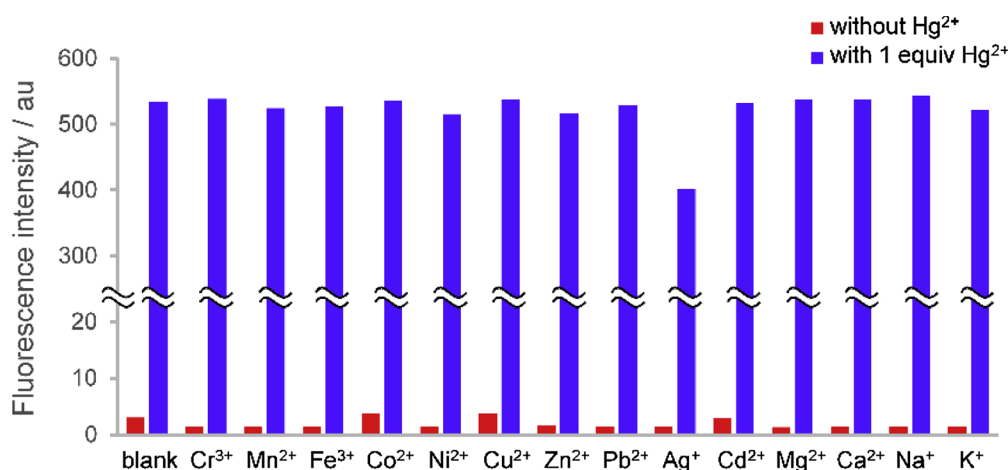**Fig. 6.** A Job's plot of the fluorescence intensities obtained in solutions of **1**, Hg^{2+}, or a mixture of **1** and Hg^{2+} versus the mole fraction [**1**]/([**1**] + [Hg^{2+}]). The total concentration ([**1**] + [Hg^{2+}]) was fixed at 5 μM, and the data were collected at λ_{ex} = 370 nm and λ_{em} = 455 nm.

Fig. 7. Effects of metal ions (5 μM Cr^{3+}, Mn^{2+}, Fe^{3+}, Co^{2+}, Ni^{2+}, Cu^{2+}, Zn^{2+}, Pb^{2+}, Ag^+ and Cd^{2+}, 0.1 mM Mg^{2+}, Ca^{2+}, Na^+ and K^+) on the fluorescence intensity of **1** (5 μM) in the absence or presence of Hg^{2+} (5 μM). The data were collected in pH 7.2 phosphate buffer containing 0.1% (v/v) DMSO at $\lambda_{ex} = 370$ nm and $\lambda_{em} = 455$ nm.

Table 1

Quantitative analysis for Hg^{2+} in tap and river water by the fluorometry with **1** (5 μM).

Spiked amount of Hg^{2+} (μM)	Recovered amount of $Hg^{2+} \pm SD^*$ (μM)	
	Tap water	River water
0	−0.00307 ± 0.00166	−0.00445 ± 0.00061
0.05	0.0442 ± 0.00071	0.0456 ± 0.00300
0.1	0.102 ± 0.00079	0.0983 ± 0.00231
0.25	0.252 ± 0.00202	0.247 ± 0.00253
0.5	0.545 ± 0.00836	0.514 ± 0.00482
1.0	1.04 ± 0.00382	1.00 ± 0.00527
2.0	1.99 ± 0.0153	1.96 ± 0.0117

* Standard deviation ($n = 3$).

For this purpose, we used virtual water samples contaminated with Hg^{2+}, that is, mixtures of tap or river water and pH 7.2 phosphate buffer (1:1, v/v) spiked with Hg^{2+} over the concentration range between 0.05 and 2 μM. The concentrations of Hg^{2+} in the samples were estimated by fluorometry using **1** (5 μM) with a calibration curve method, as shown in Table 1. The fluorometric analysis gave satisfactory results, suggesting that without any tedious pretreatments, **1** could be utilized for practical analysis of Hg^{2+} in water samples containing Hg^{2+} over the examined concentration range at least.

4. Conclusion

We have developed **1** as a fluorescent turn-on probe for Hg^{2+} by manipulating functional groups tethered to naphthalimide based on the concept provided by the previous work on a fluorescent Cd^{2+} probe. The present work demonstrated not only that **1** allows highly selective and sensitive analysis of Hg^{2+} in real water samples without any tedious pretreatment, but also that carbamoylmethylamino group tethered to naphthalimide could be a key structure to design a fluorescent turn-on probe for other metal ions. We are currently investigating further application of this concept supported by the present as well as previous works.

Acknowledgement

Appendix A. Supplementary data

Supplementary material related to this article can be found, in the online version, at doi:https://doi.org/10.1016/j.jphotochem.2018.11.034.

References

[1] C.C. Bridges, R.K. Zalups, Transport of inorganic mercury and methylmercury in target tissues and organs, J. Toxicol. Environ. Health B Crit. Rev. 13 (2010) 385–410.
[2] R.K. Zalups, Molecular interactions with mercury in the kidney, Pharmacol. Rev. 52 (2000) 113–144.
[3] E.M. Nolan, S.J. Lippard, Tools and tactics for the optical detection of mercuric ion, Chem. Rev. 108 (2008) 3443–3480.
[4] P.L. Goering, D.L. Morgan, S.F. Ali, Effects of mercury vapor inhalation on reactive oxygen species and antioxidant enzymes in rat brain and kidney are minimal, J. Appl. Toxicol. 22 (2002) 167–172.
[5] A. Stacchiotti, F. Morandini, F. Bettoni, I. Schena, A. Lavazza, P.G. Grigolato, P. Apostoli, R. Rezzani, M.F. Aleo, Stress proteins and oxidative damage in a renal derived cell line exposed to inorganic mercury and lead, Toxicology 264 (2009) 215–224.
[6] M.J.H. Worthington, R.L. Kucera, I.S. Albuquerque, C.T. Gibson, A. Sibley, A.D. Slattery, J.A. Campbell, S.F.K. Alboaiji, K.A. Muller, J. Young, N. Adamson, J.R. Gascooke, D. Jampaiah, Y.M. Sabri, S.K. Bhargava, S.J. Ippolito, D.A. Lewis, J.S. Quinton, A.V. Ellis, A. Johs, G.J.L. Bernardes, J.M. Chalker, Laying waste to mercury: inexpensive sorbents made from sulfur and recycled cooking oils, Chem. Eur. J. 23 (2017) 16219–16230.
[7] Y. Yang, Q. Zhao, W. Feng, F. Li, Luminescent chemodosimeters for bioimaging, Chem. Rev. 113 (2013) 192–270.
[8] B.P. Joshi, C.R. Lohani, K.-H. Lee, A highly sensitive and selective detection of Hg (II) in 100% aqueous solution with fluorescent labeled dimerized Cys residues, Org. Biomol. Chem. 8 (2010) 3220–3226.
[9] W. Lin, X. Cao, Y. Ding, L. Yuan, Q. Yu, A reversible fluorescent Hg^{2+} chemosensor based on a receptor composed of a thiol atom and an alkene moiety for living cell fluorescence imaging, Org. Biomol. Chem. 8 (2010) 3618–3620.
[10] J. Du, J. Fan, X. Peng, P. Sun, J. Wang, H. Li, S. Sun, A new fluorescent chemodosimeter for Hg^{2+}: selectivity, sensitivity, and resistance to Cys and GSH, Org. Lett. 12 (2010) 476–479.
[11] Y. Zhou, C.-Y. Zhu, X.-S. Gao, X.-Y. You, C. Yao, Hg^{2+}-Selective ratiometric and "off-on" chemosensor based on the azadiene-pyrene derivative, Org. Lett. 12 (2010) 2566–2569.
[12] G. Aragay, H. Montón, J. Pons, M. Font-Bardía, A. Merkoçi, Rapid and highly sensitive detection of mercury ions using a fluorescencebased paper test strip with an *N*-alkylaminopyrazole ligand as a receptor, J. Mater. Chem. 22 (2012) 5978–5983.
[13] X. Ma, J. Wang, Q. Shan, Z. Tan, G. Wei, D. Wei, Y. Du, A "turn-on" fluorescent Hg^{2+} chemosensor based on ferrier carbocyclization, Org. Lett. 14 (2012) 820–823.
[14] R. Pandey, M. Yadav, M. Shahid, A. Misra, D.S. Pandey, Design and synthesis of fluorescent 6-aryl[1,2-c]quinazolines serving as selective and sensitive 'on-off' chemosensor for Hg^{2+} in aqueous media, Tetrahedron Lett. 53 (2012) 3550–3555.
[15] W.-Y. Liu, S.-L. Shen, H.-Y. Li, J.-Y. Miao, B.-X. Zhao, Fluorescence turn-on chemodosimeter for rapid detection of mercury (II) ions in aqueous solution and blood from mice with toxicosis, Anal. Chim. Acta 791 (2013) 65–71.
[16] C. Wang, K.M.-C. Wong, Selective Hg^{2+} sensing behaviors of rhodamine derivatives with extended conjugation based on two successive ring-opening processes, Inorg. Chem. 52 (2013) 13432–13441.
[17] N. Kumari, N. Dey, S. Jha, S. Bhattacharya, Ratiometric, reversible, and parts per billion level detection of multiple toxic transition metal ions using a single probe in micellar media, ACS Appl. Mater. Interfaces 5 (2013) 2438–2445.
[18] L. Song, Z. Lei, B. Zhang, Z. Xu, Z. Li, Y. Yang, A zero-background fluorescent probe for Hg^{2+} designed via the "covalent-assembly" principle, Anal. Methods 6 (2014)

7597–7600.

[19] H.-I. Un, C.-B. Huang, C. Huang, T. Jia, X.-L. Zhao, C.-H. Wang, L. Xu, H.-B. Yang, A versatile fluorescent dye based on naphthalimide: highly selective detection of Hg^{2+} in aqueous solution and living cells and its aggregation-induced emission behavior, Org. Chem. Front. 1 (2014) 1083–1090.

[20] J. Ding, H. Li, C. Wang, J. Yang, Y. Xie, Q. Peng, Q. Li, Z. Li, "Turn-on" fluorescent probe for mercury(II): high selectivity and sensitivity and new design approach by the adjustment of the π-bridge, ACS Appl. Mater. Interfaces 7 (2015) 11369–11376.

[21] H. Lin, W. Shi, Y. Tian, F. Ma, L. Xu, J. Ma, Y. Hui, Z. Xie, A simple and highly selective 'turn-on' type fluorescence chemodosimeter for Hg^{2+} based on 1-(2-phenyl-2H-[1,2,3]triazole-4-carbonyl)thiosemicarbazide, J. Lumin. 157 (2015) 280–284.

[22] S. Choi, Y. Kim, Gold nanoparticle-based fluorescent "turn-on" sensing system for the selective detection of mercury ions in aqueous solution, RSC Adv. 5 (2015) 95268–95272.

[23] H. Xiao, J. Li, K. Wu, G. Yin, Y. Quan, R. Wang, A turn-on BODIPY-based fluorescent probe for Hg(II) and its biological applications, Sens. Actuators B Chem. 213 (2015) 343–350.

[24] L.N. Neupane, E.-T. Oh, H.J. Park, K.-H. Lee, Selective and sensitive detection of heavy metal ions in 100% aqueous solution and cells with a fluorescence chemosensor based on peptide using aggregation-induced emission, Anal. Chem. 88 (2016) 3333–3340.

[25] D. Li, C.-Y. Li, Y.-F. Li, Z. Li, F. Xu, Rhodamine-based chemodosimeter for fluorescent determination of Hg^{2+} in 100% aqueous solution and in living cells, Anal. Chim. Acta 934 (2016) 218–225.

[26] J. García-Calvo, S. Vallejos, F.C. García, J. Rojo, J.M. García, T. Torroba, A smart material for the *in situ* detection of mercury in fish, Chem. Commun. (Camb.) 52 (2016) 11915–11918.

[27] Z. Zhong, D. Zhang, D. Li, G. Zheng, Z. Tian, Turn-on fluorescence sensor based on naphthalene anhydride for Hg^{2+}, Tetrahedron 72 (2016) 8050–8054.

[28] Q. Zhang, J. Zhang, H. Zuo, C. Wang, Y. Shen, A novel near-infrared chemosensor for mercury ion detection based on D-A structure of triphenylamine and benzothiadiazole, Tetrahedron 73 (2017) 2824–2830.

[29] S.-L. Pan, K. Li, L.-L. Li, M.-Y. Li, L. Shi, Y.-H. Liu, X.-Q. Yu, A reaction-based ratiometric fluorescent sensor for the detection of Hg(II) ions in both cells and bacteria, Chem. Commun. (Camb.) 54 (2018) 4955–4958.

[30] P.A. Panchenko, Y.V. Fedorov, O.A. Fedorova, Selective fluorometric sensing of Hg^{2+} in aqueous solution by the inhibition of PET from dithia-15-crown-5 ether receptor conjugated to 4-amino-1,8-naphthalimide fluorophore, J. Photochem. Photobiol. A: Chem. 364 (2018) 124–129.

[31] X. Cheng, S. Qu, L. Xiao, W. Li, P. He, Thioacetalized coumarin-based fluorescent probe for mercury(II): ratiometric response, high selectivity and successful bioimaging application, J. Photochem. Photobiol. A: Chem. 364 (2018) 503–509.

[32] S. Qin, B. Chen, J. Huang, Y. Han, A thiocoumarin-based colorimetric and ratiometric fluorescent probe for Hg^{2+} in aqueous solution and its application in live-cell imaging, New J. Chem. 42 (2018) 12766–12772.

[33] K. Tsukamoto, S. Shimabukuro, M. Mabuchi, H. Maeda, A naphthalimide-based Cd^{2+} fluorescent probe with carbamoylmethyl groups working as chelators and PET-promoters under neutral conditions, Chem. Eur. J. 22 (2016) 8579–8585.

[34] D.F. Eaton, Reference materials for fluorescence measurement, Pure Appl. Chem. 60 (1988) 1107–1114.

[35] N.J. Turro, V. Ramamurthy, J.C. Scaiano, Principles of Molecular Photochemistry: An Introduction, University Science Books, California, 2009, pp. 311–313.

[36] X. Wang, L. Andrews, Infrared spectrum of $Hg(OH)_2$ in solid neon and argon, Inorg. Chem. 44 (2005) 108–113.